Burnette et al., http://www.jcb.org/cgi/content/full/jcb.201311104/DC1

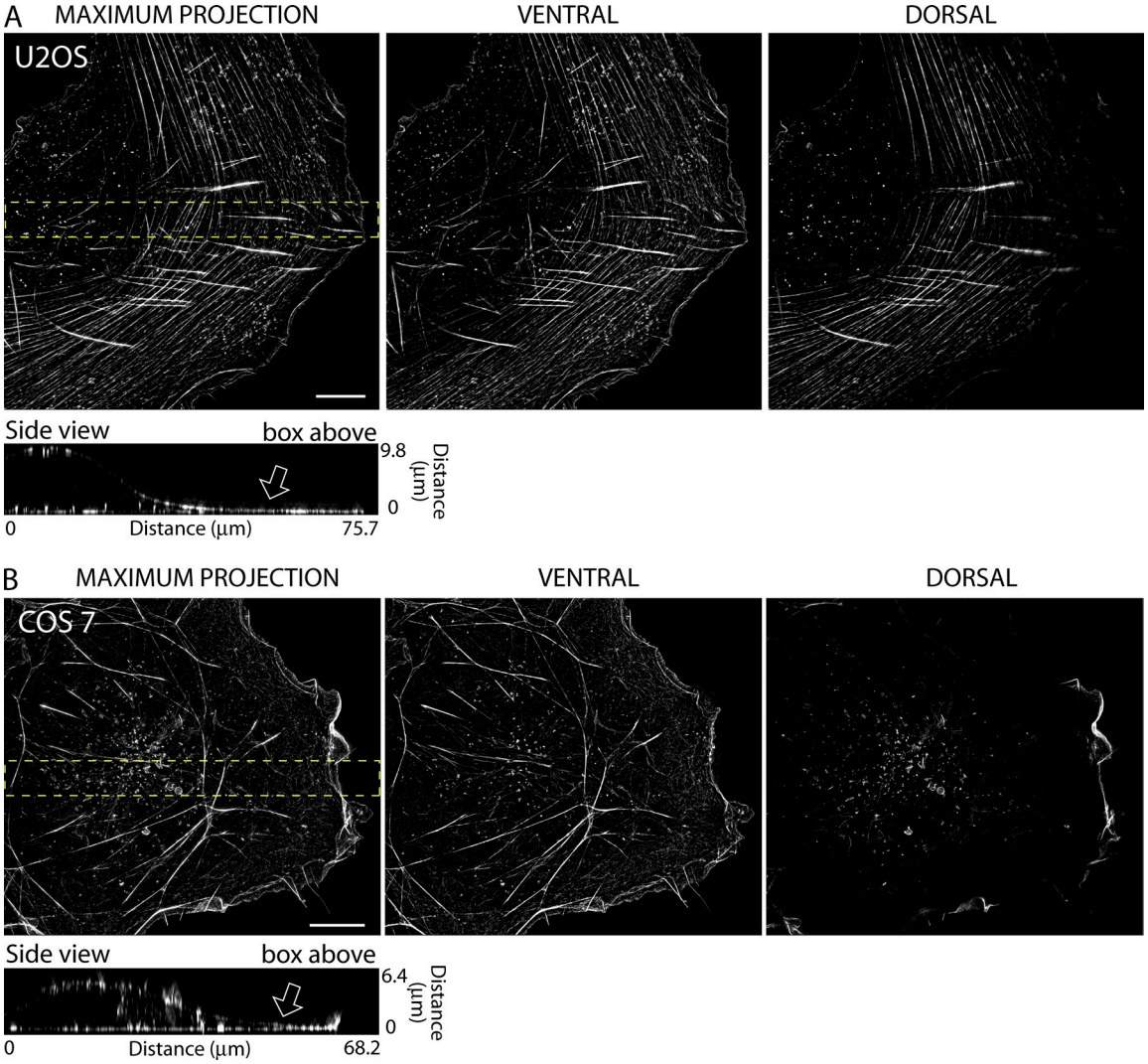

Figure S1. **Protocols that extract membranes before fixation flatten the lamella.** (A and B) Actin filaments stained with phalloidin–Alexa Fluor 488 in a U2OS cell (A) and a Cos7 cell (B) after a live-cell extraction (see Materials and methods) followed by fixation. Maximum projections, dorsal views, and ventral views are shown. Side views were created as an x-z projection of the boxes shown in the maximum projection images. Note that both U2OS cells have flat lamella that contain a single SIM-resolvable layer of actin filaments in the vertical dimension (see white arrows in side views). In U2OS cells, the ventral and dorsal actin filament layers are collapsed. Although not dramatic, this flattening of the lamella is significant because this collapse precludes SIM's ability to resolve the ventral and dorsal networks. While flattening of U2OS cells is apparent, the flattening of Cos7 cells is even more dramatic (B). After live-cell extraction, the shape of a Cos7 cell is similar to a U2OS cell; both have a very flat leading edge where ventral and dorsal actin networks are not resolvable. However, the edge of Cos7 cells are typically microns tall (Fig. 9), not <100 nm in height, as it is after a live-cell extraction treatment as seen in B.

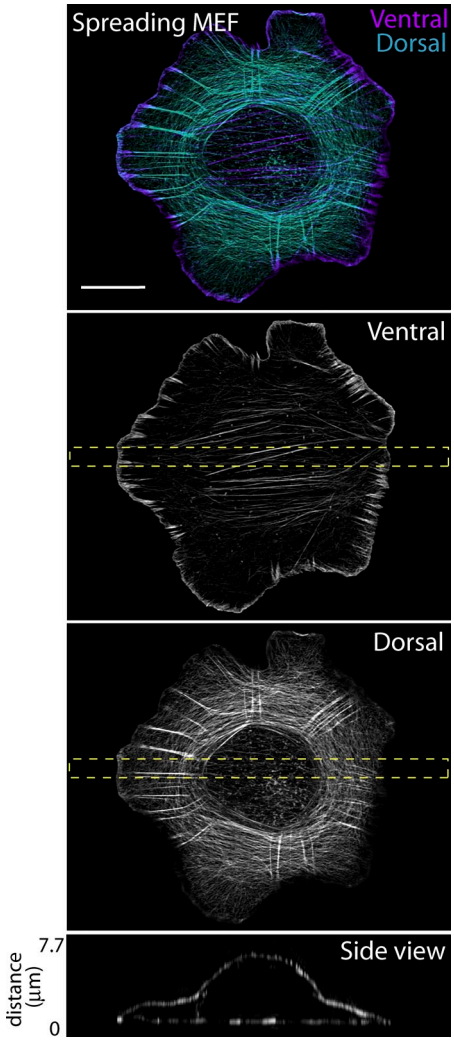

Figure S2. **An isolated spreading MEF cell has ventral/dorsal actin filament organization similar to cells polarized by cell–cell contact.** Cells in this study were chosen based on two criteria: (1) they had a symmetrical curved leading edge and (2) they contacted another cell at their rear. This ensured that each cell had similar stress fiber organization (e.g., all of stress fibers on the surface of the cells were "arc shaped") and the cells were polarized, respectively. However, even when cells are not polarized by cell contact, such as in the case of an isolated MEF cell spreading out, we observed a conserved structure. Shown here are the ventral and dorsal views of a MEF that has been spreading for 30 min. Note the presence of ventral stress fibers in the ventral view and DSFs/actin arcs in the dorsal view. The side view was generated by a z-x maximum projection from the region denoted by the yellow boxes. Bar, 10 μm.

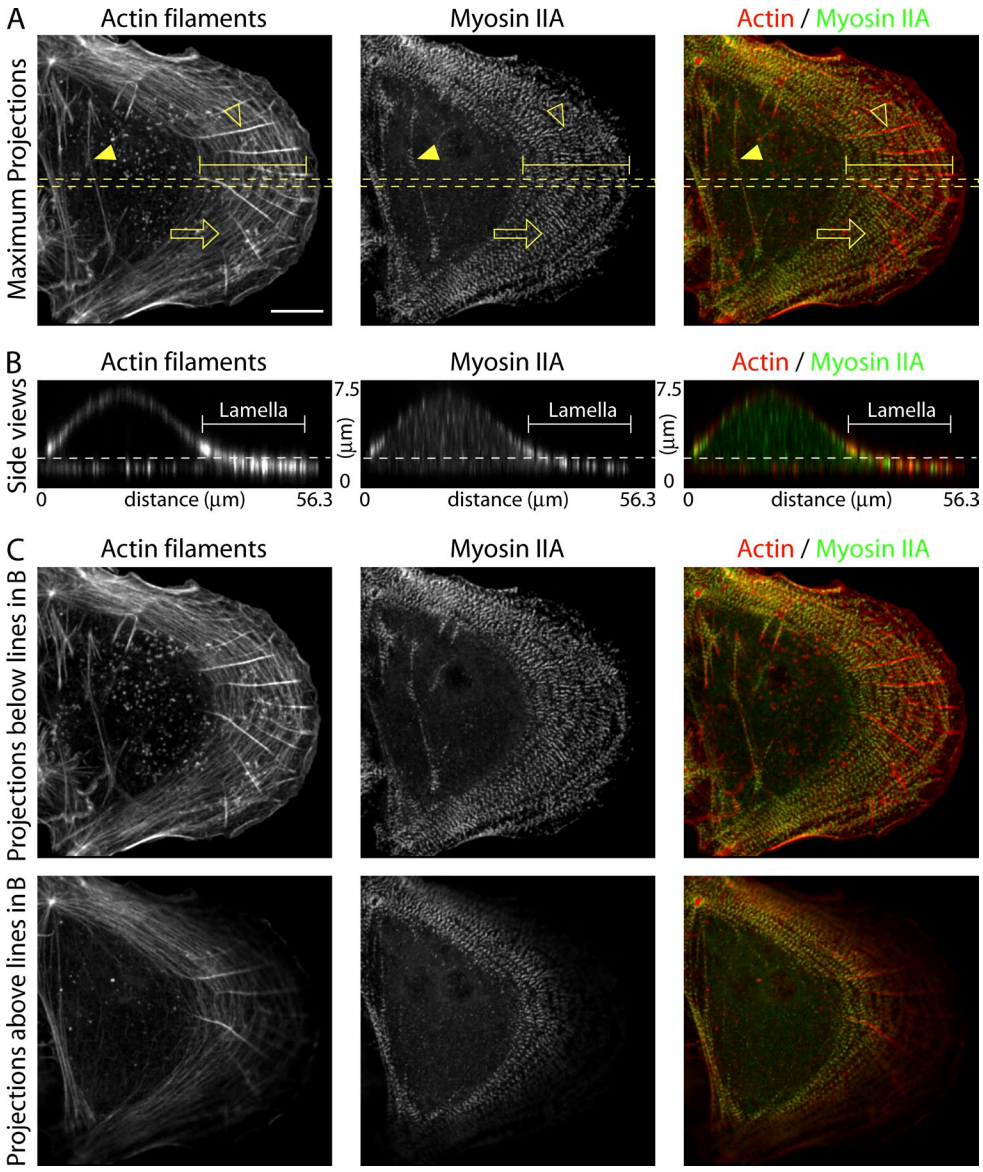

Figure S3. **Endogenous localization of myosin IIA.** (A–C) Maximum-projection images from confocal z series of the U2OS cell shown in Fig. 1 (A–C), showing actin filaments (phalloidin–Alexa Fluor 488) and immunolocalized endogenous myosin IIA (Alexa Fluor 568 secondary) and an overlay. (A) Open arrows, open arrowheads, and closed arrowheads denote actin arcs, DSF, and ventral stress fibers, respectively. Brackets denote lamella. (B) Side views of the boxes in A. Brackets denote lamella and dotted lines denote the axially diffraction–limited layer at the bottom of the cell. (C) x-y maximum projections from below and above the dotted line in B. Note that although some ends of DSFs and myosin II–laden actin arcs can be seen in projection above the line in B, the majority are contained within the axially diffraction-limited region on the cell's bottom. Bar, 10 μm.

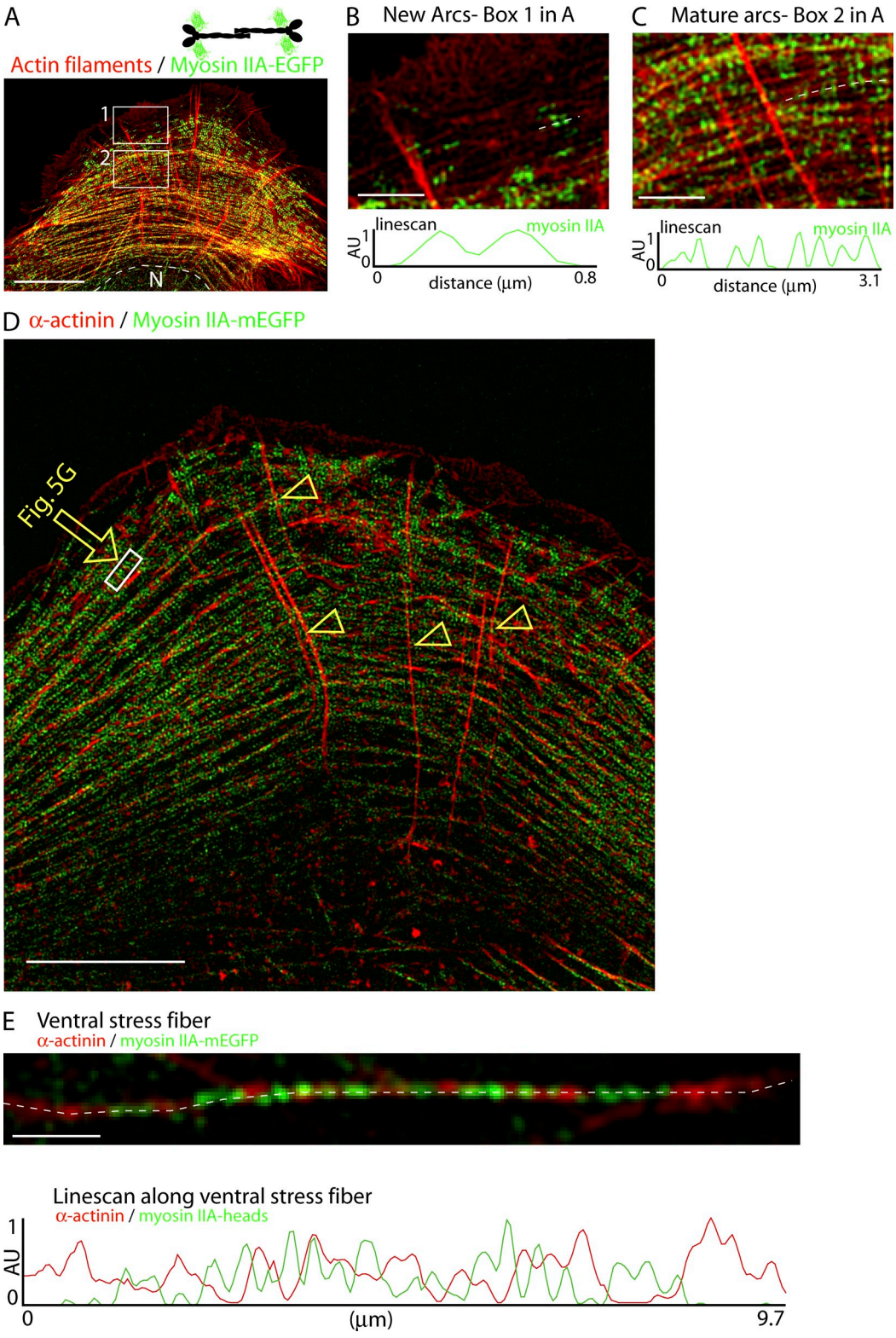

Figure S4. **SIM of myosin IIA–mEGFP motor domains and actin filaments.** (A) Maximum projection of actin filaments (TRITC-phalloidin) and myosin II–mEGFP expressed in a U2OS cell. The schematic shows a myosin II filament labeled with heavy chains fused to mEGFP on their N-termini incorporated into it. (B and C) Higher magnification of box 1 (B) and box 2 (C) from the image in A. (B) Myosin II incorporated into nascent actin arcs is oriented with their long axis parallel to the leading edge. (C) Myosin II stacks in mature actin arcs are also oriented parallel to the leading edge. (D) Low-magnification image of α-actinin and myosin II motor domains. SIM of α-actinin–mApple (red) and myosin II–mEGFP (green) in a U20S cell is shown. The white box denotes the region shown in Fig. 5 G. Arrowheads denote α-actinin localized to DSFs. (E) SIM of α-actinin and myosin IIA along a ventral stress fiber. α-actinin–mApple and myosin IIA–mEGFP are shown in red and green, respectively. It was difficult to resolve myosin II motor domains of individual filaments along ventral stress fibers, as shown by the graph of the signals along the dotted line in the image. We particularly did not find the α-actinin and myosin II motor domain pattern as seen on the dorsal side of the cell. Bars: (A) 10 μm; (B and C) 2 μm; (D) 10 μm; (E) 1 μm.

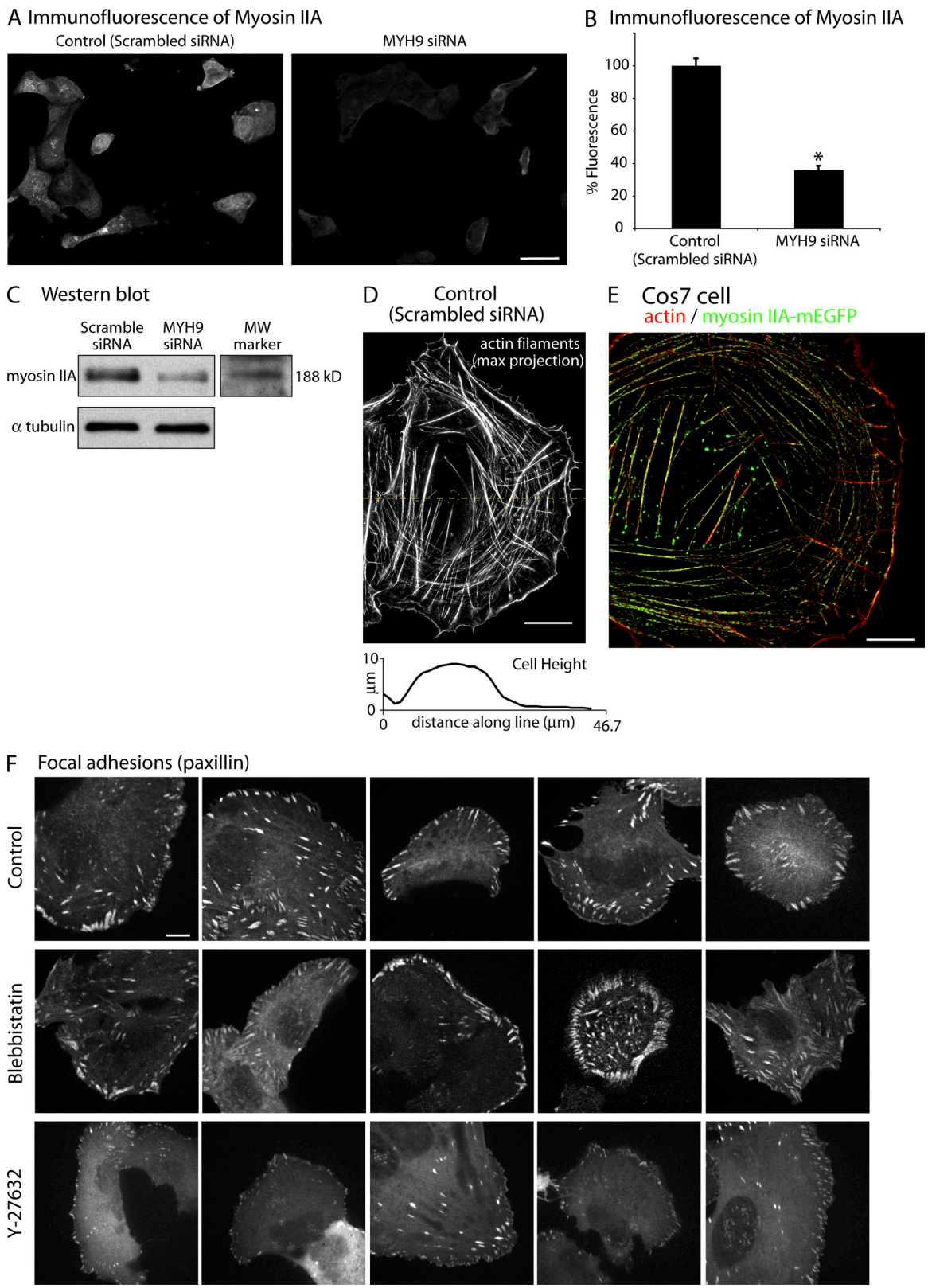

Figure S5. **siRNA of MYH9 in U2OS cells and expression of myosin IIA in Cos7 cells.** (A) Immunofluorescence of myosin IIA in U2OS cells treated with either a scrambled siRNA control or MYH9 siRNA. Bar, 50 µm. (B) Quantification of reduction of immunofluorescent signal between control and MYH9 siRNA. Fluorescence was normalized for cell area and presented as a percent of the control's mean. (C) Western blot showing myosin IIA levels in cells treated with scramble or MYH9 siRNA. α-Tubulin was used as a loading control. (D) SIM of actin filaments from a cell treated with scrambled siRNA (maximum projection). Note that the scrambled siRNA did not remove actin arcs or change the flatness of the lamella. Note the presence of DSFs/actin arcs and a normal cell height profile. (E) Myosin IIA localized in a Cos7 cell. Maximum projection of the myosin IIA–mApple (green) and actin filaments (Alexa Fluor 488–phalloidin) from the cell shown in Fig. 9 B. (F) Change in focal adhesions after removal of actin arcs and DSF. Focal adhesions were visualized by expression of paxillin-EGFP in U2OS cells. Control cells (top), and cells treated with either 20 µM blebbistatin (middle), or 10 µM Y-27632 (bottom) for 2 h are shown. Very little difference in focal adhesion morphology was found in cells treated with the low levels of blebbistatin, whereas, as reported by Oakes et al. (2012), focal adhesions were reduced in 10 µM Y-27632. As both drug treatments abolish the flatness of the lamella, changes in focal adhesions do not appear to be required for this shape change. Myosin IIA and actin were pseudo-colored green and red, respectively, to remain consistent with the data displayed in the rest of this article. Bars: (A) 50 µm; (D–F) 10 µm.

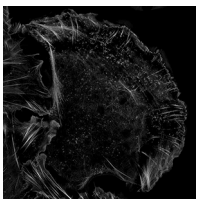

Video 1. **Actin filament layers in a U2OS cell.** This movie shows z sections from the SIM of the actin filaments from the U2OS cell shown in Fig. 2. The cell was fixed with 4% paraformaldehyde, and actin filaments were labeled with Alexa Fluor 488–phalloidin and imaged using a SIM microscope (Elyra; Zeiss Carl Zeiss). Sections through 6.6 µm in the z dimension with 110-nm steps between images are shown. Video scale: horizontal, 76.2 µm; vertical, 76.0 µm.

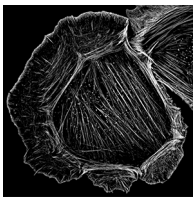

Video 2. **Actin filament layers in a MEF cell.** This movie shows z sections from the SIM of the actin filaments from the MEF cell shown in Fig. 3. The cell was fixed with 4% paraformaldehyde, and actin filaments were labeled with Alexa Fluor 488–phalloidin and imaged using a SIM microscope (Elyra; Zeiss Carl Zeiss). Sections through 6.6 µm in the z dimension with 110-nm steps between images are shown. Video scale: horizontal, 60.7 µm; vertical, 61.7 µm.

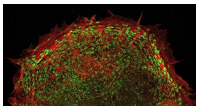

Video 3. **SIM of myosin IIA and α-actinin in a live U2OS cell.** This movie shows a time-lapse recording of myosin IIA–mEmerald (green) and α-actinin–mApple (red) transiently expressed in U2OS cells. The time lapse was acquired at 37°C in L15 medium with a custom-designed SIM microscope, as described in the Materials and methods. A maximum projection of each channel was created to create the overlay shown here. Video length, 11 min, 15 s. Video scale: horizontal, 22.4 µm; vertical, 42.5 µm.

Reference

Oakes, P.W., Y. Beckham, J. Stricker, and M.L. Gardel. 2012. Tension is required but not sufficient for focal adhesion maturation without a stress fiber template. *J. Cell Biol.* 196:363–374. http://dx.doi.org/10.1083/jcb.201107042